

Observation of a non-Ohmic Hall resistivity above the critical temperature in the high-temperature superconductor $\text{YBa}_2\text{Cu}_3\text{O}_{7-\delta}$

I. Puica* and W. Lang†

*Fakultät für Physik, Universität Wien,
Boltzmanngasse 5, A-1090 Wien, Austria*

K. Siraj, J. D. Pedarnig, and D. Bäuerle

Institut für Angewandte Physik, Johannes-Kepler-Universität Linz, A-4040 Linz, Austria

Abstract

Investigations of the resistivity and the Hall effect as a function of electric field and temperature in the normal state and upper part of the superconducting transition of an optimally doped, very thin film of $\text{YBa}_2\text{Cu}_3\text{O}_{7-\delta}$ are reported. Using a fast pulsed-current technique allowed to reduce the self-heating of the sample and to reach electric fields up to 1 kV/cm. An intrinsic non-Ohmic behavior of the Hall conductivity above the critical temperature that appears to originate from two different, partially counteracting effects is revealed. The major contribution stems from the suppression of Aslamazov-Larkin superconducting fluctuations in high electric fields.

I. INTRODUCTION

The non-linear behavior of the normal-state resistivity close to the superconducting transition was studied about three decades ago in the conventional superconductors both theoretically,^{1,2,3} and experimentally on thin aluminum films,^{4,5} and good agreement between experiment and theory was found. The mechanism for this effect was explained in terms of a change of the paraconductivity that is evoked by thermodynamic superconducting fluctuations. A sufficiently high electric field can accelerate the fluctuating paired carriers so that, on a distance of the order of the coherence length, they increase their energy by a value corresponding to the fluctuation Cooper pair binding energy. This results in an additional, electric field dependent, decay mechanism and leads to deviation of the current-voltage characteristics from Ohm's law.

In the high-temperature cuprate superconductors (HTSC) many physical properties including the fluctuation spectrum are significantly different due to the small coherence lengths and the strongly anisotropic layered structures of these materials.⁶ Several investigations of a non-Ohmic in-plane conductivity above T_c have been reported and attributed to the paraconductivity suppression in high electric fields.^{7,8,9,10} Such measurements suffer from an inherent self-heating of the samples that needs to be properly addressed. A satisfactory agreement with the theoretical models for layered superconductors based on a microscopic approach¹¹ or on the time-dependent Ginzburg-Landau (TDGL) theory^{12,13} has been found only with reduction and correction of the self-heating¹⁴ using a pulsed current technique^{9,14} and additionally very thin films.^{10,15}

The influence of high current densities on the Hall effect has been investigated in HTSC,^{16,17,18,19,20} with the aim of overcoming the vortex pinning and testing its influence on the Hall anomaly that is observed below T_c . An intrinsic non-Ohmic effect above T_c was neither explicitly investigated nor fortuitously found in these studies. A possible reason is that the applied currents did not exceed 10^6 Acm⁻², while theoretical estimates for the suppression of superconducting fluctuations²¹ indicate a rather small effect on the Hall conductivity that might need even higher current densities to be observed.

In this paper we present our recent investigations of the Hall effect in $\text{YBa}_2\text{Cu}_3\text{O}_{7-\delta}$ (YBCO) above and close to T_c in high electric fields, performed with a pulsed-current technique^{10,15} that enables significantly higher current densities than have been previously

applied in Hall effect measurements.^{16,18} Our aim is to look for non-Ohmic effects on the Hall conductivity in the upper part of the superconducting transition region, and to test whether these effects could be explained as a consequence of the fluctuation suppression in strong electric fields. The results can contribute important information to the long-lasting debate on the origin of the Hall anomaly in HTSC.²²

II. SAMPLE PREPARATION AND EXPERIMENTAL SETUP

In this work we present resistivity and Hall effect data from an optimally doped *c*-axis-oriented epitaxial YBCO film with a thickness of 50 nm and with $T_c = 86.8$ K. The measurements were checked for reproducibility on a second film with similar results. Our films were prepared by pulsed-laser deposition²³ on MgO substrates and patterned by standard photolithography and wet-chemical etching into a bridge geometry of 200 μ m length and 50 μ m width with two arms at 100 μ m distance on each side for the voltage probes. The current contacts were located more than 3 mm apart from the bridge.

Longitudinal and transverse voltages were collected at the same time using a pulsed-current technique, whose electric scheme is detailed elsewhere.^{10,15} Two identical circuits were used for the measurement of the longitudinal and transverse voltages. The electric potentials relative to ground at the sample probes were connected to the inputs of differential amplifiers with very high common mode rejection ratio (100000:1 up to $f = 100$ kHz, decreasing proportional to $1/f$ for higher frequencies). Their output signals were transmitted to the two channels of a high-resolution (14 bit) digitizer, sampled at a 200 MHz rate, averaged and recorded for further analysis. A possible deterioration of the transverse voltage signal due to an insufficient common mode rejection of the differential amplifier at high frequencies was overcome by the symmetrical arrangement of the apparatus with respect to ground, with two identical programmable pulse generators of opposite polarity. The common mode voltage is thus of the order of the differential signal. The other parts of the experimental setup consisted of a closed-cycle refrigerator and an electromagnet. The polarity of the 0.8 T magnetic field was reversed multiple times for every data point, and for every magnetic field value the longitudinal and transverse voltage pulses were simultaneously recorded.

The duration of the square-wave current pulses used in our measurements was 3.5 μ s, at a repetition frequency of 16 Hz, so that the cumulative heating between subsequent pulses

could be avoided. Moreover, for pulse duration of the order of μs , the thermal diffusion distance in the film is of the order of tens of microns at a quench velocity of about 10 m/s,²⁴ so that heat generated at the current contacts (which are a few mm distant from the bridge) does not interfere with the measurement.

The pulse length is, on the other hand, long enough to establish a flat plateau of the voltage signal after the initial transient state, and voltage values could be recorded in a well resolved time-window of about 1 μs length in the last third of the pulse duration. This time-window contained about 200 sampled instant values, whose average gave the voltage value for the respective pulse. To increase the signal-to-noise ratio, 1024 subsequent pulses were averaged, allowing for a measurement precision better than $\pm 1 \mu\text{V}$ for the Hall voltage and better than $\pm 10 \mu\text{A}$ for the current. The measurements were performed at discrete temperature values, measured at the sample holder with a stability better than $\pm 0.01 \text{ K}$.

The main source of the remaining sample heating during the short high-current pulses is the limited heat transfer across the film-substrate interface, which occurs with a characteristic phonon escape time of the order of 1 ns, $\tau_{es} = R_b c_p d$, with d the film thickness, R_b the thermal boundary resistance, and c_p the phonon specific heat of the film.²⁵ To overcome this effect the measurement would have to be performed in sub-ns time after the current onset, which is out of scope for this kind of measurement. At the interface to the substrate arises thus an abrupt temperature difference between an apparent temperature T_a measured at the heat sink (sample holder) and the higher sample temperature T :¹⁴

$$T - T_a \approx p d R_b \quad (1)$$

where p is the dissipated power density in the sample. According to Eq. 1, the temperature rise can be reduced by a proper choice of d and R_b . Hence, we have used as thin as possible samples that still exhibit a T_c close to the bulk value and MgO as substrate, for its lower thermal resistance as against Al₂O₃ or LaAlO₃.²⁵

The interface between YBCO and MgO exhibits different kinds of imperfections, like structural defects and modifications of the local charge density, which both can reduce the conductivity of the film in the vicinity of the interface. The intrinsic properties are recovered only at some distance from the substrate boundary. This defect-rich zone exhibits a substantially higher resistance, the linear temperature characteristics of the normal-state resistance is distorted, and T_c suppressed. It typically extends about 10 to 30 nm from

the interface into the YBCO film and has been verified by resistivity measurements and transmission electron microscopy.^{26,27} To account for this situation in our ultra-thin film we consider an ‘effective electrical thickness’ of the YBCO film that corresponds to the thickness of the undistorted top layer. The higher resistivity of our sample as compared to thicker films prepared under otherwise identical conditions can be thus ascribed to an effective thickness of the film that is smaller than the geometrical one. For our 50 nm thick films, an effective electrical thickness of about 30 nm was assumed. It should be emphasized that a possible error in the thickness has no influence on the conclusions regarding a non-Ohmic behavior.

III. RESULTS AND DISCUSSION

The longitudinal and the Hall resistivities of our YBCO thin film are presented in Figs. 1 and 2, respectively. Data were taken with the pulse technique described above at fixed sample holder temperatures T_a with variation of the injected current and, consequently, the applied electric field. At very low fields the values measured with the pulse technique approach the values of a conventional DC measurement (filled symbols), thus, proving the consistency between the two measurement methods.

The pulse-current technique allowed to attain unprecedented electric fields of almost 1000 V/cm, current densities as high as 12 MAcm^{-2} (at the rightmost point of the $T_a = 79 \text{ K}$ curve in Fig. 1) and dissipated power densities of more than 11 GWcm^{-3} (for instance at the highest electric field at $T_a = 140 \text{ K}$) without damaging the sample.

However, as one can see from Figs. 1 and 2, a resistivity increase and, respectively, a Hall resistivity decrease with higher electric fields is present even for temperatures deep in the normal state, e.g., at $T_a = 140 \text{ K}$ or $T_a = 127 \text{ K}$, where the fluctuation contribution should be vanishingly small. A non-Ohmic effect from hot electrons like it was observed in many semiconductors²⁸ is unlikely due to the low carrier mobilities in the HTSC. A straightforward explanation is a temperature increase in the sample, caused by excessive dissipation and the finite thermal boundary resistance at the film-substrate interface according to Eq. 1. In order to account for this self-heating by applying a temperature correction, we first derive the temperature dependence of the longitudinal and Hall resistivity at constant electric field from the experimental data, shown in Figs. 3 and 4, respectively.

In order to eliminate the spurious effects of self-heating we use Eq. (1) to estimate the

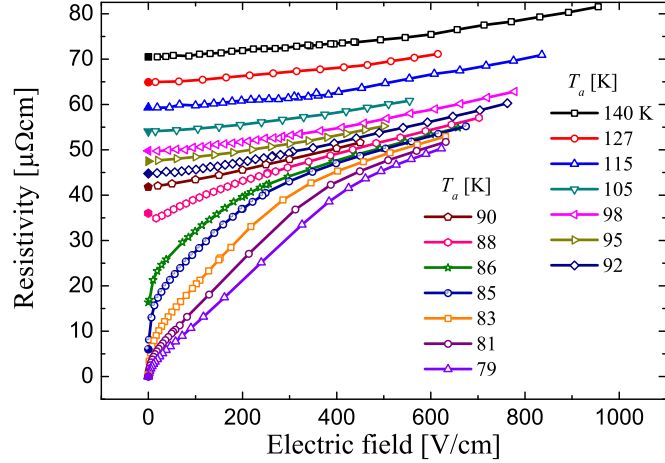


FIG. 1: (color online). Resistivity of a thin YBCO film measured with $3.5 \mu\text{s}$ current pulses (open symbols and solid lines) at different fixed sample holder temperatures T_a as a function of the applied electric field. Measurement accuracy is better than $\pm 0.5 \mu\Omega\text{cm}$ (disregarding the uncertainty of the sample geometrical dimensions, which enter only as scaling factors in the absolute values of resistivity and electric field). A magnetic field $B = 0.8 \text{ T}$ was applied perpendicular to the film surface. The filled symbols show the corresponding resistivity values measured with low DC current.

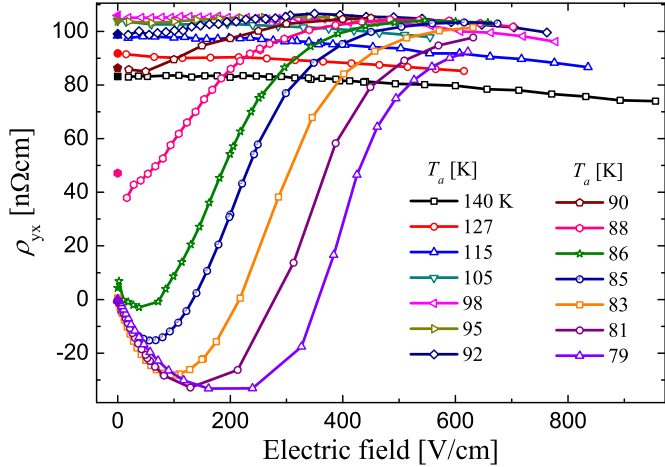


FIG. 2: (color online). Hall resistivity measured simultaneously with the resistivity from Fig. 1 with pulsed currents (open symbols and solid lines) and with low DC current (filled symbols). Measurement accuracy is better than $\pm 1 \text{ n}\Omega\text{cm}$ (disregarding the uncertainty of the sample geometrical dimensions).

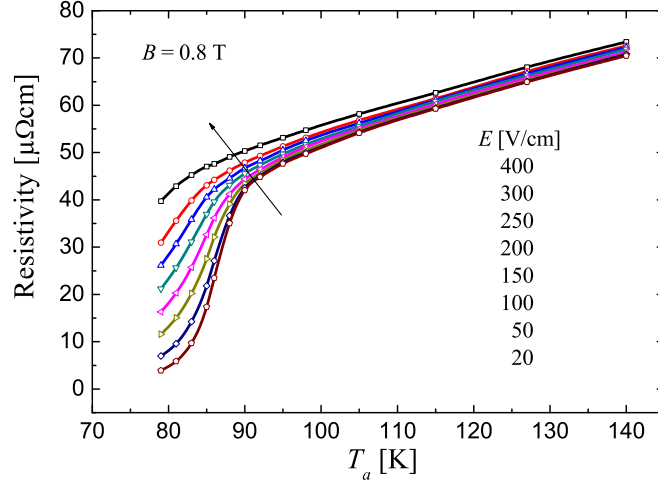


FIG. 3: (color online). Resistivity, derived from data of Fig. 1, as a function of the sample holder temperature at various constant electric fields. The arrow indicates the sequence of increasing electric fields.

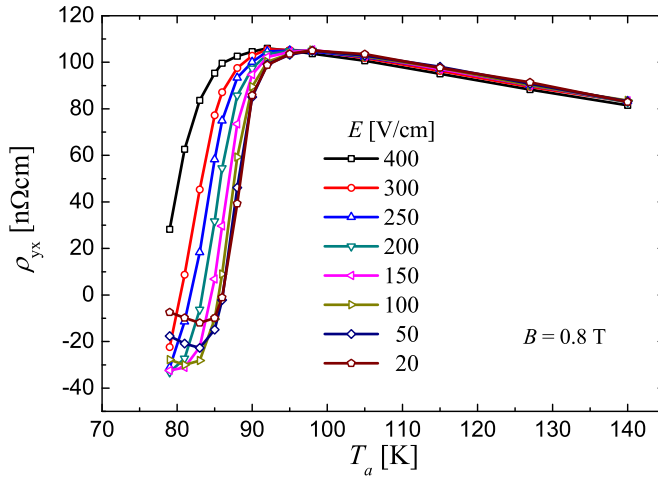


FIG. 4: (color online). Hall resistivity, derived from data of Fig. 2, as a function of the sample holder temperature at various constant electric fields.

sample temperature at each individual data point. The thermal boundary resistance R_b is chosen as a constant fit parameter in such way that all the resistivity curves superpose in the normal state, up to an uncertainty represented by the curve thickness. An appropriate value is $R_b = 0.7$ mKcm²W⁻¹, a value typical for a YBCO/MgO interface.^{25,29} Possible shortcomings of this method could be for instance the assumption that R_b is independent of temperature, temperature drop, and transferred power density at the film-substrate in-

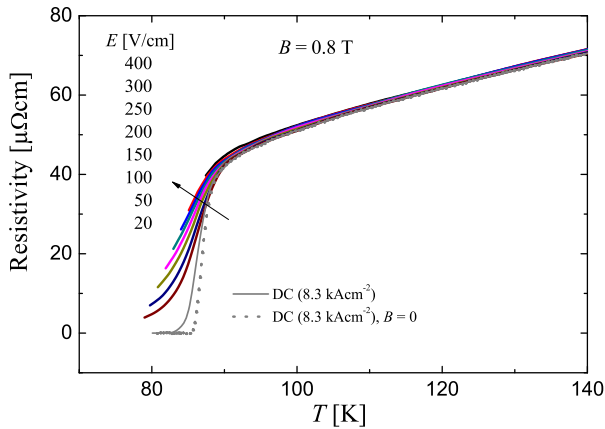


FIG. 5: (color online). Resistivity data (thick solid lines) from Fig. 3 according to Eq. 1. For reference, the resistivity measured at a low DC current is also shown, in $B = 0.8$ T (thin solid gray line) and at $B = 0$ (dotted gray line). The arrow indicates the sequence of increasing electric fields. The uncertainty of the corrected temperature is comparable to the curve thickness.

terface. The thermal boundary resistance was found indeed to be almost independent on temperature and heat flux density,^{29,30} but also with some slight decrease with substrate temperature²⁵ and heat flux³¹ above T_c . Since our analysis is limited to a narrow temperature range such higher-order corrections should not be important and, if they have an influence at all, they would increase the non-linearities of the Hall resistivity around 90 K that are discussed below. Finally, the resistivity and the Hall resistivity are independent quantities with opposite temperature variations in the normal state, and the fact that the very same temperature correction reduces both of them to the low-current characteristics strongly indicates the self-heating as the only significant effect for nonlinear behavior at high electric fields deep in the normal state.

The temperature-corrected resistivity data from Fig. 5 exhibit the fan-shape broadening of the superconducting transition at increasing electric fields, which was also previously experimentally observed^{9,10,14,15} and attributed to (at least in the high-temperature part of the transition) the suppression of superconducting fluctuations.¹³

At first sight, it appears that the Hall resistivity in Fig. 6 is Ohmic not only in the normal state, but in the entire region, where $\rho_{yx} > 0$, i.e., down to temperatures where the Hall effect changes its sign. A weak effect can be seen near the maximum of ρ_{yx} , where the curve

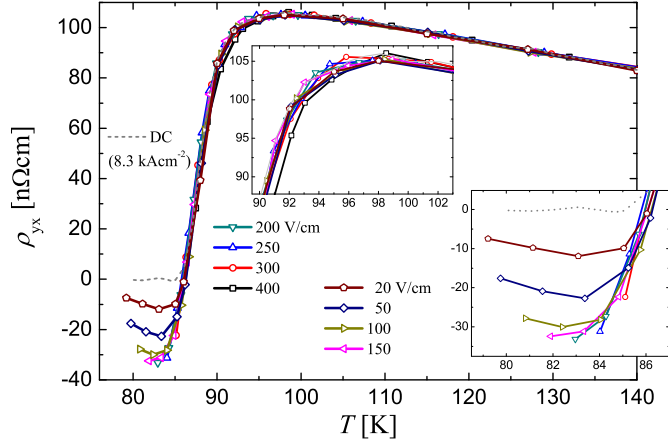


FIG. 6: (color online). Hall resistivity data from Fig. 4, re-scaled by the same temperature correction as in Fig. 5. The dotted curve is the Hall resistivity measured at low DC current. The insets show details of the Hall resistivity maximum and its negative minimum, respectively.

changes to a lower slope (see inset of Fig. 6). It is important to realize that the temperature region $T < 90$ K, where a significant non-Ohmic effect appears in the resistivity, corresponds to the very steep region of the ρ_{yx} curve and, thus, any small change cannot be seen in the graph. On the other hand, the almost perfect collapse of the curves in the steep region means that there is only vanishing uncertainty about the sample temperature, an additional indication of the validity of our temperature correction procedure.

A very strong non-Ohmic effect can be noticed in the region of $\rho_{yx} < 0$, where the negative minimum is dramatically enhanced at higher electric fields. A similar behavior has been observed previously — although in smaller current densities than in the present work — and has been attributed to the fact that pinning forces are overcome in elevated current densities.^{16,18} Our present results for this temperature region do agree with those conclusions and reveal additional effects that becomes noticeable in extremely high current densities. This effects are better evidenced in the Hall conductivity picture, as it is shown below.

It has been proposed by several groups that the Hall conductivity $\sigma_{xy} = \rho_{yx}/(\rho_{yx}^2 + \rho_{xx}^2)$ should be appropriate for an analysis of the Hall effect in the vicinity of T_c since several effects contribute additively and σ_{xy} is believed to be almost independent of pinning.³² This picture is shown in Fig. 7 and, since the curves also have intrinsically a smaller slope, it allows for a better visualization of the non-Ohmic Hall effect.

One can now notice two counteracting effects of a high electric field on the Hall conduction

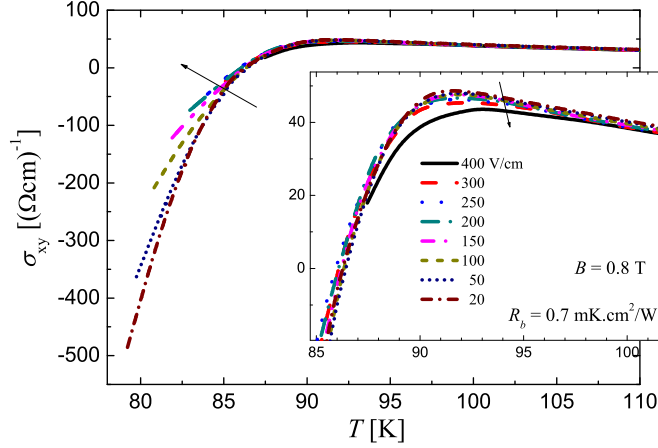


FIG. 7: (color online). Hall conductivity computed from data of Figs. 5 and 6. The region around the maximum Hall conductivity is shown on a larger scale in the inset. The arrows indicate the sequence of increasing electric field. The accuracy of the Hall conductivity is better than $\pm 3 \Omega^{-1}\text{cm}^{-1}$ (disregarding the uncertainty of the sample geometrical dimensions). The low-temperature cutoff of the curves is caused by the high-current limits and the resulting temperature corrections.

tivity. The first one is a softening of the drop of σ_{yx} (Fig. 7) that resembles qualitatively the fan-shape broadening observed for the resistivity (Fig. 5). Such a non-Ohmic dependence of the Hall conductivity has been recently theoretically predicted in the frame of the TDGL equation,²¹ based on a suppression of the superconducting fluctuation lifetime. The behavior displayed in Fig. 7 is in good qualitative correspondence with the theoretical one, but the magnitude of the effect is somewhat smaller, possibly also due to the second effect that will be discussed below.

Some brief remarks on the sign reversal of the Hall effect and its connection with our present data is appropriate here. The essential features of the sign reversal and of the Hall anomaly are known to be governed by a negative contribution to the Hall conductivity that originates already at $T > T_c$ and apparently diverges towards lower temperatures. It leads to both the sharp drop of the Hall resistivity and to its sign change.^{17,33,34,35,36} The negative contribution to σ_{xy} is frequently ascribed, both by theoretical and experimental work, to fluctuating superconducting pairs, essentially to those of the Aslamazov-Larkin (AL) process.^{37,38,39,40,41} The Hall resistivity, however, does not diverge towards lower temperatures, but, on the contrary, vanishes. This can be understood by the fact that $\rho_{yx} = \sigma_{xy} / (\sigma_{xx}^2 + \sigma_{xy}^2) \simeq \sigma_{xy} \rho_{xx}^2$ is dominated in this temperature range by the behavior of

$\rho_{xx} \rightarrow 0$. By the same consideration, the enhancement of the negative Hall anomaly in Fig. 6 turns out to be essentially due to the non-Ohmic effect on the *longitudinal* resistivity ρ_{xx} that is increased with the electric field, since the change of the Hall conductivity of Fig. 7, whose negative value diminishes in magnitude in high electric fields, would have an opposite effect on the Hall resistivity. Hence, although a non-Ohmic behavior of the Hall resistivity can be seen at low temperatures, the effects under investigation here are obscured in this quantity.

The second effect on the Hall conductivity is better discernible in the inset of Fig. 7. The maximum of σ_{xy} slightly diminishes with increasing fields and this reduction extends more than $T_c + 10$ K into the normal state. It is emphasized that σ_{xy} has almost no temperature dependence in this region, so that an artifact from self-heating or improper temperature correction can be ruled out. Also, this effect appears to be weaker temperature dependent than the suppression of AL-type fluctuations discussed before and has the opposite direction, so that it counteracts the effect displayed in the main panel of Fig. 7.

We know of no direct prediction of such an effect but would like to discuss some possible origins. In earlier works on the fluctuation Hall conductivity under Ohmic conditions an additional Maki-Thompson (MT) contribution^{42,43} was included to obtain a fit to the experimental data.^{37,44} The anomalous MT fluctuation term cannot be treated in the phenomenological TDGL theory, and, to our best knowledge, no microscopic theory for the high electric field effect on the MT contribution is available. It can be tentatively assumed that the suppression of superconducting fluctuations by a high electric field would also reduce the MT contribution to the Hall conductivity. Since the MT term has the same positive sign as the normal state part and a weaker temperature dependence as compared to the AL term, such a suppression of MT fluctuations could evoke the behavior displayed in the inset of Fig. 7. On the other hand, the *d*-wave pairing symmetry in HTSC is known to suppress the MT process,^{45,46,47,48} so that the MT contribution to the Hall conductivity and consequently to its high electric field change could be rather negligible.

Another contribution can result from the reduction of density of states (DOS) when carriers condense into fluctuating pairs⁶ or as a result of the pseudogap. The former effect has some similarities with the MT contribution, but so far has been not explicitly observed experimentally in the Hall effect of HTSC. A speculative pseudogap effect can be expected to be rather small in our near-optimally doped samples, but might be nevertheless worth men-

tioning, considering that the observed effect extends only to a few kelvin above T_c . Clearly, further theoretical and experimental studies are needed to provide possible explanations of this novel effect.

IV. CONCLUSIONS

In summary, we have investigated the non-Ohmic effects on the resistivity and the Hall effect in optimally doped very thin films of YBCO using a fast pulsed-current technique. The sample self-heating could be significantly reduced so that measurements with current densities of more than 10 MAcm^{-2} and high electric fields up to almost 1 kV/cm in the normal state were possible. We have found evidence of an intrinsic non-Ohmic behavior of the Hall conductivity above the critical temperature that appears to originate from two different, partially counteracting effects. One of these could be identified as the suppression of Aslamazov-Larkin superconducting fluctuations in high electric fields.

Acknowledgments

This work was supported by the Austrian Science Fund (FWF) and the Research Network ‘Nanoscience and Engineering in Superconductors (NES)’ of the European Science Foundation. We appreciate enlightening discussions with A. A. Varlamov and T. Mishonov.

* Electronic address: ionut.puica@univie.ac.at

† Electronic address: wolfgang.lang@univie.ac.at

¹ A. Schmid, Phys. Rev. **180**, 527 (1969).

² J. P. Hurault, Phys. Rev. **179**, 494 (1969).

³ T. Tsuzuki, Progr. Theoret. Phys. (Kyoto) **43**, 286 (1970).

⁴ G. A. Thomas and R. D. Parks, Physica **55**, 215 (1971).

⁵ K. Kajimura, N. Mikoshiba, and K. Yamaji, Phys. Rev. B **4**, 209 (1971).

⁶ A. I. Larkin and A. Varlamov, *Theory of Fluctuations in Superconductors*, no. 127 in International Series of Monographs on Physics (Clarendon Press, Oxford, 2005).

⁷ J. C. Soret, L. Ammor, B. Martinie, J. Lecomte, P. Odier, and J. Bok, *Europhys. Lett.* **21**, 617 (1993).

⁸ I. G. Gorlova, S. G. Zybtshev, and V. I. Pokrovskii, *JETP Lett.* **61**, 839 (1995).

⁹ L. Fruchter, I. Sfar, F. Bouquet, Z. Z. Li, and H. Raffy, *Phys. Rev. B* **69**, 144511 (2004).

¹⁰ W. Lang, I. Puica, M. Peruzzi, L. Lemmermann, J. D. Pedarnig, and D. Bäuerle, *phys. stat. sol. (c)* **2**, 1615 (2005).

¹¹ A. A. Varlamov and L. Reggiani, *Phys. Rev. B* **45**, 1060 (1992).

¹² T. Mishonov, A. Posazhennikova, and J. Indekeu, *Phys. Rev. B* **65**, 064519 (2002).

¹³ I. Puica and W. Lang, *Phys. Rev. B* **68**, 054517 (2003).

¹⁴ M. N. Kunchur, *Mod. Phys. Lett. B* **9**, 399 (1995).

¹⁵ I. Puica, W. Lang, M. Peruzzi, K. Lemmermann, J. D. Pedarnig, and D. Bäuerle, *Supercond. Sci. Technol.* (2004).

¹⁶ M. N. Kunchur, D. K. Christen, C. E. Klabunde, and J. M. Phillips, *Phys. Rev. Lett.* **72**, 2259 (1994).

¹⁷ T. W. Clinton, A. W. Smith, Q. Li, J. L. Peng, R. L. Greene, C. J. Lobb, M. Eddy, and C. C. Tsuei, *Phys. Rev. B* **52**, R7046 (1995).

¹⁸ W. Liebich, P. Gehringer, W. Göb, W. Lang, K. Bierleutgeb, and D. Bäuerle, *Physica C* **282-287**, 2321 (1997).

¹⁹ K. Nakao, K. Hayashi, T. Utagawa, Y. Enomoto, and N. Koshizuka, *Phys. Rev. B* **57**, 8662 (1998).

²⁰ W. Göb, W. Liebich, W. Lang, I. Puica, R. Sobolewski, R. Rössler, J. D. Pedarnig, and D. Bäuerle, *Phys. Rev. B* **62**, 9780 (2000).

²¹ I. Puica and W. Lang, *Phys. Rev. B* **70**, 092507 (2004).

²² I. Puica, W. Lang, W. Göb, and R. Sobolewski, *Phys. Rev. B* **69**, 104513 (2004).

²³ D. Bäuerle, *Laser Processing and Chemistry, 3rd Edition* (Springer, Berlin, Heidelberg, 2000).

²⁴ A. Heinrich, *Supercond. Sci. Technol.* **18**, 1354 (2005).

²⁵ A. V. Sergeev, A. D. Semenov, P. Kouminov, V. Trifonov, I. G. Goghidze, B. S. Karasik, G. N. Gol'tsman, and E. M. Gershenzon, *Phys. Rev. B* **49**, 9091 (1994).

²⁶ T. Venkatesan, X. D. Wu, B. Dutta, A. Inam, M. S. Hedge, D. M. Hwang, C. C. Chang, L. Nazar, and B. Wilkens, *Appl. Phys. Lett.* **54**, 581 (1989).

²⁷ J. D. Pedarnig, R. Rössler, M. P. Delamare, W. Lang, D. Bäuerle, A. Köhler, and H. W.

Zandbergen, *Appl. Phys. Lett.* **81**, 2587 (2002).

²⁸ N. Balkan, *Hot Electrons in Semiconductors: Physics and Devices* (Oxford University Press, 1998).

²⁹ M. Nahum, S. Verghese, P. L. Richards, and K. Char, *Appl. Phys. Lett.* **59**, 2034 (1991).

³⁰ K. Harrabi, N. Cheene, F. Chibane, F. Boyer, P. Delord, F. Ladan, and J. Maneval, *Supercond. Sci. Technol.* **13**, 1222 (2000).

³¹ M. Kelkar, P. Phelan, and B. Gu, *Int. J. Heat Mass Transfer* **40**, 2637 (1997).

³² V. M. Vinokur, V. B. Geshkenbein, M. V. Feigelman, and G. Blatter, *Phys. Rev. Lett.* **71**, 1242 (1993).

³³ J. P. Rice, N. Rigakis, D. M. Ginsberg, and J. M. Mochel, *Phys. Rev. B* **46**, 11050 (1992).

³⁴ W. N. Kang, D. H. Kim, S. Y. Shim, J. H. Park, T. S. Hahn, S. S. Choi, W. C. Lee, J. D. Hettinger, K. E. Gray, and B. Glagola, *Phys. Rev. Lett.* **76**, 2993 (1996).

³⁵ Y. Matsuda, T. Nagaoka, G. Suzuki, K. Kimagai, M. Suzuki, M. Machida, M. Sera, M. Hiroi, and N. Kobayashi, *Phys. Rev. B* **52**, R15749 (1995).

³⁶ J. Roa-Rojas, P. Prieto, and P. Pureur, *Mod. Phys. Lett.* **15**, 1117 (2001).

³⁷ W. Lang, G. Heine, P. Schwab, X. Z. Wang, and D. Bäuerle, *Phys. Rev. B* **49**, 4209 (1994).

³⁸ A. V. Samoilov, A. Legris, F. Rullier-Albenque, P. Lejay, S. Bouffard, Z. G. Ivanov, and L.-G. Johansson, *Phys. Rev. Lett.* **74**, 2351 (1995).

³⁹ A. W. Smith, T. W. Clinton, W. Liu, C. C. Tsuei, A. Pique, Q. Li, and C. J. Lobb, *Phys. Rev. B* **56**, R2944 (1997).

⁴⁰ J. M. Graybeal, J. Luo, and W. R. White, *Phys. Rev. B* **49**, 12923 (1994).

⁴¹ D. A. Beam, N. C. Yeh, and F. Holtzberg, *J. Phys.: Condens. Matter* **10**, 5955 (1998).

⁴² K. Maki, *Prog. Theor. Phys.* **39**, 897 (1968).

⁴³ R. S. Thompson, *Phys. Rev. B* **1**, 327 (1970).

⁴⁴ R. L. Neiman, J. Giapintzakis, D. M. Ginsberg, and J. M. Mochel, *J. Supercond.* **8**, 383 (1995).

⁴⁵ S. Yip, *Phys. Rev. B* **41**, 2612 (1990).

⁴⁶ P. Carretta, A. Rigamonti, A. A. Varlamov, and D. V. Livanov, *Phys. Rev. B* **54**, R9682 (1996).

⁴⁷ M. V. Ramallo, A. Pomar, and F. Vidal, *Phys. Rev. B* **54**, 4341 (1996).

⁴⁸ M. T. Béal-Monod and K. Maki, *Europhys. Lett.* **33**, 309 (1996).